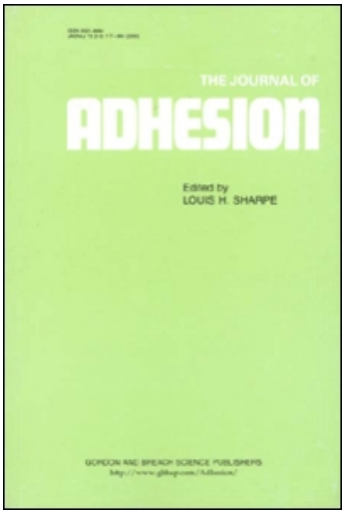

The Journal of Adhesion

Publication details, including instructions for authors and subscription information:
http://www.informaworld.com/smpp/title~content=t713453635

A Method to Measure the Adhesion of Thin Glass Coatings on Polymer Films

Y. Leterrier[a]; Y. Wyser[a]; J. A. E. Månson[a]; J. Hilborn[bc]
[a] Département des Matériaux, Laboratoire de Technologie des Composites et Polyméres, Lausanne, Switzerland [b] Pharmacia Hospital Care, Stockholm, Sweden [c] Département des Matériaux, Laboratoire de Polyméres, Lausanne, Switzerland

To cite this Article Leterrier, Y. , Wyser, Y. , Månson, J. A. E. and Hilborn, J.(1994) 'A Method to Measure the Adhesion of Thin Glass Coatings on Polymer Films', The Journal of Adhesion, 44: 3, 213 — 227
To link to this Article: DOI: 10.1080/00218469408027078
URL: http://dx.doi.org/10.1080/00218469408027078

J. Adhesion, 1994, Vol. 44, pp. 213–227
Reprints available directly from the publisher
Photocopying permitted by license only

A Method to Measure the Adhesion of Thin Glass Coatings on Polymer Films

Y. LETERRIER, Y. WYSER, J. -A. E. MÅNSON*

Laboratoire de Technologie des Composites et Polymères, Département des Matériaux, Ecole Polytechnique Fédérale de Lausanne, CH-1015 Lausanne, Switzerland

and

J. HILBORN**

Pharmacia Hospital Care, Franséngatan 6, S-112 87 Stockholm, Sweden

(Received December 13, 1993; in final form March 17, 1994)

A simple and reliable method to measure the adhesion of thin, hard coatings on polymer substrates is presented, based on the rupture mechanics of brittle films on ductile substrates. The regular fragmentation pattern of the coating obtained after straining specimens under uniaxial tension is analyzed through a classical shear-lag analysis at the coating/substrate interface. The model links the mean crack spacing measured on strained specimens to the interfacial shear strength and the reversible adhesion energy. Fragmentation tests were carried out on a PET film coated on both sides by SiO_2 layers (24 nm on the thick side, and 6 nm on the thin side). The interfacial shear strength was found to be close to 100 MPa for both coatings and the adhesion energy of SiO_2 on PET was found to be of the order of 230 mJ/m^2, both values being slightly higher for the thin coating side.

KEY WORDS glass coating; adhesion; fragmentation pattern; stress transfer; interfacial shear strength; reversible adhesion energy; PET; SiO_2 layers; CVD coating.

INTRODUCTION

The integrity of the coating is often a crucial factor in determining the performance of a coated component. Adhesion to the substrate is one of the most important properties of the coating, since the quality of this interaction controls the durability of the device. Modern deposition techniques, such as chemical vapor deposition, were originally developed in the microelectronic industry for SiO_x and AlO_x amorphous thin films, to achieve high adhesion levels. Specifically, flexible, transparent, recyclable, thin film gas barriers were lately designed, and are now widely discussed in the packaging industry.[1,2] Active research is presently being carried out to improve the reliability of these new materials, with the quality of the adhesion of the barrier layer as a key issue.[3]

* Corresponding author.
** Present address: Laboratoire de Polymères, Département des Matériaux, Ecole Polytechnique Fédérale de Lausanne, CH-1015 Lausanne, Switzerland.

Moreover, the effect of variations in the application process and the prediction of performance is often based on adhesion measurements.

The measure of the interfacial adhesion of thin coatings has received considerable attention in the past decades. Indeed, among numerous adhesion tests, at least eight different quantitative techniques were reviewed.[4-11] Among these, indentation testing, scratch testing and acoustic microscopy have emerged as the most appropriate methods of adhesion measurement of thin, hard coatings.[7,9,10,12] The indentation test introduces a mechanically-stable crack into the coating-substrate interface, and is able to generate high stresses that exceed the interfacial bond strength of thin and well-adhering coatings.[7] The test assumes that the interface, in the vicinity of the plastic zone created in the substrate during indentation, possesses a lower toughness than either coating or substrate and, therefore, will be a site of lateral crack formation.[10] The scratch test is derived from the indentation test, and yields a more quantitative measure of film adhesion.[12] Considerable progress has been made for the scratch test regarding the relationship between the work of adhesion and the critical load for coating removal for hard coatings on soft substrates. Nevertheless, there is still room to develop theoretical work to take into account the effects of coating thickness and coating material. As detailed in extensive reviews for this specific test, only an accurate description of the stress field associated with the indenter displacement will enable a reliable measure of the adhesion strength.[7,9,10] Up to now there is still a requirement for an ideal method, and a promising route is likely to be acoustic microscopy.[10] This technique, developed to image the elastic properties of bulk polymer composite materials,[13] is mainly used to detect defects and areas of poor adhesion at the coating-substrate interface.[14] Acoustic microscopy is still considered as an efficient means to image adhesion quality at an interface, although the frequencies in the acoustic microscope are much higher than those of typical viscoelastic processes in polymers, which would limit the application of the technique to only the aspects of adhesion controlled by elasticity.[15]

Alternatively, we have developed a method, derived from the cracking phenomena in thin films, that may be considered as a reliable technique to measure the adhesion performance of thin and brittle coatings on ductile substrates. Remarkable fragmentation patterns in brittle films adhering to high elongation substrates are common natural manifestations (*e.g.*, mud-cracking). Together with considerable improvements in coating technologies, intense research has been carried out to investigate the mechanics of rupture of thin, hard coatings on a wide variety of substrates.[8,16-22] Numerous studies have focused on the specific case of multiple parallel cracking of the coating resulting from uniaxial elongation of the substrate. This pure geometry allows a good control of the stress field generated in the material during its elongation, in a manner similar to the classical single fiber fragmentation test originally designed by Kelly and Tyson,[23] now widely used to measure the interfacial shear strength in fiber-reinforced polymer composites.[24-28] In both coating/substrate and fiber/matrix geometries, the modeling of the load transfer at the interface is a typical shear-lag analysis.[29] This classical theory has proved to be efficient in the case of thin films on ductile substrates.[20] All these approaches have in common multiple fractures of one of the components in a strained composite structure.[19,30] Furthermore, the straining of

coated polymer films is likely to become the most suitable method to examine the evolution of the properties of various coatings, such as the gas transmission rate.[3]

The aims of this work are twofold: i) to apply the fragmentation technique to the case of a glass-coated thermoplastic polymer and to measure the crack spacing distribution at saturation and, ii) to derive expressions for the interfacial shear strength from simple stress transfer analysis[20,23] and for the reversible work of adhesion, based on recent adhesion analysis.[31-33]

EXPERIMENTAL

The material investigated in the present study was a 12 μm thick poly(ethylene terephthalate) (PET) film, coated with a thin SiO_2 layer (Airco, CA, USA). Plasma-enhanced chemical vapor desposition (CVD) was used to produce amorphous and highly inorganic glass coatings on the PET substrate.[1,2] Compared with evaporation processes, this specific technique is a cold process and prevents to a large extent thermal loading of the PET substrate.[1] Therefore, it was assumed that the polymer surface had not been affected during the process, though no measure of the surface temperature was available. In the present case, the film had been coated on both sides in an on-line operation, giving material supplied in roll form.

The mechanical behavior of the glass-coated film was measured under uniaxial tension. Rectangular specimens ($100 \times 10\,mm^2$) were cut from the film, along the roll direction, or perpendicular to the roll direction. Tension tests were performed on an Adamel Lhomargy DY-30 machine, at a constant crosshead speed of 1 mm/min. All experiments were carried out at room temperature, and four tests were realized for each type of specimen. The tension force, F, was recorded as a function of the crosshead displacement, d, from which was deduced the nominal tension stress, $\sigma = F/S_o$ and the nominal strain, $\varepsilon = d/l_o$, S_o and l_o being the initial specimen cross section ($0.12\,mm^2$) and length (25 mm), respectively. The strain rate was $6.7 \times 10^{-4}\,s^{-1}$.

The morphology of the glass coating was subsequently analyzed under scanning electronic microscopy (SEM), on samples cut from parallel tension specimens subjected to a strain of 0.2. SEM samples with non-conductive surfaces such as glasses are first usually coated with a thin gold layer. In order to prevent any artifacts arising from the possible tearing of the gold layer under the electron beam, the JEOL JSM 6300 SEM was operated at low voltage (1 kV) with non gold-coated samples. Both the thick and the thin glass sides of each sample were examined. The crack spacing distribution at saturation (*i.e.*, when the crack density becomes constant) of the glass coatings obtained after straining the films was measured from SEM photographs using an image analysis system IBAS (Kontron Electronic).

Electron spectroscopy for chemical analysis (ESCA) was also used to determine the chemical composition of the SiO_2/PET interface using an Ar^+ ionic bombardment. The difference and standard deviation of binding energies between O_{1s} and Si_{2p} during successive Ar^+ sputtering steps were used for the calculation of the stoichiometry and the detection of the interface. The SiO_2 coating thickness was deduced from the examination of an effective surface area of $0.2\,mm^2$, on four samples.[34]

RESULTS

Glass Coating Thicknesses

ESCA experiments confirmed that the PET film was coated on both sides. On one side the layer was found to be 24 nm thick, whereas on the other side the layer was 6 nm thick. The thickness of the thicker coating (which is controlled during the deposition process) was found to be 25.8 $\pm$ 1.5 nm by the manufacturer using X-ray fluorescence, in good agreement with our measure. A typical error of 10% is usually considered in the measurement of thicknesses of thin coatings using ESCA.[34] A simple error calculation shows that the thickness ratio is within the range 4 $\pm$ 0.56, that is, an error of 14% on the nominal value of 4. In the following, the 24 nm coating will be referred as the "thick" side, and the 6 nm coating as the "thin" side.

Mechanical Behavior of the Glass Coated PET Film

The nominal stress *vs* nominal strain curves for specimens taken both parallel and perpendicular to the roll direction are presented in Figure 1. The two types of specimens exhibit very similar behaviors with an initial elastic response, followed by a plastic flow, up to a strain to rupture close to 22%. As reported in Table I, the elastic modulus is higher for the perpendicular specimens, and close of 4 GPa for both types. The yield occurs at a strain close to 0.03, for a stress close to 90 MPa. Some plastic hardening is noticed for the perpendicular specimens.

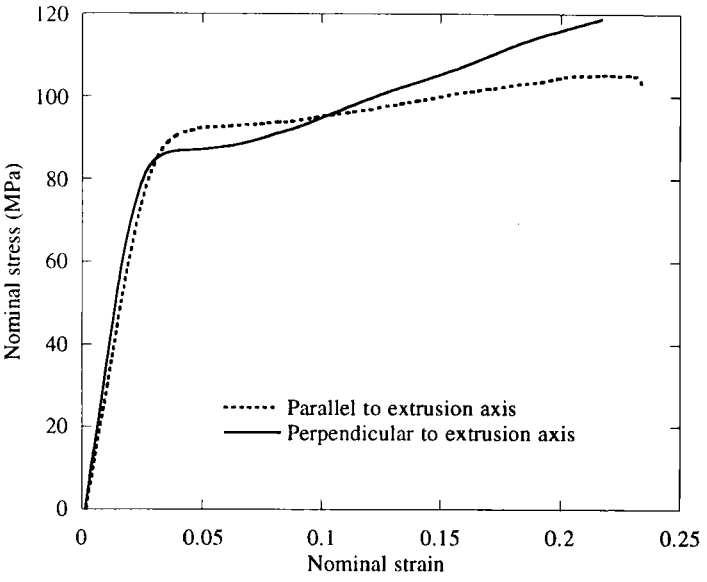

FIGURE 1 Nominal stress *vs* nominal strain for glass-coated PET film specimens cut parallel and perpendicular to the roll direction. Each curve is the average of four specimens.

TABLE I
Mechanical properties of the glass coated PET film subjected to uniaxial tension. The values reported are the average over four tests

Tension direction related to the roll	Elastic modulus (MPa)	Yield stress (MPa)	Yield strain (%)
Parallel	3,910 ± 470	91.3 ± 3.3	3.1 ± 0.1
Perpendicular	4,240 ± 350	85.8 ± 1.7	2.5 ± 0.1

From these values, the elastic modulus and the yield stress of the PET substrate were calculated following the classical rule of mixtures, *e.g.*, for the elastic modulus:

$$E_{\text{film}} = (h_g \cdot E_g + h_p \cdot E_p)/(h_g + h_p) \tag{1}$$

E_{film}: elastic modulus of the coated film
E_g : elastic modulus of the glass coating
E_p : elastic modulus of the PET substrate
h_g : glass coating thickness
h_p : PET substrate thickness

Using $E_{\text{film}} = 3910\,\text{MPa}$ for the parallel direction $h_g = 6\,\text{nm} + 24\,\text{nm} = 30\,\text{nm}$, $h_p = 12\,\mu\text{m}$, $E_g = 72.9\,\text{GPa}$ for SiO_2[35], yields $E_p = 3740\,\text{MPa}$. This result is in good agreement with typical values for PET.[36] Similarly, the yield stress of the PET was found to be 84 MPa. In this calculation, the coating strength was taken as equal to 3000 MPa, as an approximate maximum value for SiO_2.[37]

Fragmentation Morphology of the Glass Coating

Figures 2 and 3 show typical fragmentation patterns for the thick and thin glass sides, respectively, of the same specimen, subjected to 20% strain. Since careful observations of non-strained specimens did not reveal any fragmentation of the coating, it is obvious that such a regular pattern is a consequence of the uniaxial tension of the film.

Several features appear on both patterns. The main effect of straining the glass coating is the rupture of parallel strips, perpendicular to the loading direction, as is usually observed in similar experiments.[19-21] Another effect provokes the rupture of these strips into rectangular fragments, as can be seen in Figure 2. This secondary fragmentation process results from the contraction of the film perpendicular to the loading direction, controlled by the Poisson's ratio of the PET.[19] This contraction leads to a rupture under compression of the coating strips. This mechanism appears clearly in Figure 4, which presents an enlarged image of overlapping glass fragments. A careful examination of the fragmentation behavior shows that the separation of the strips starts before the film contracts. However, as indicated by the arrow in Figure 2, both rupture phenomena (coating fragmentation into parallel strips, and breakage of strips into rectangular fragments) occur simultaneously after some loading time. Indeed, cracks parallel to the strip direction appear on several strips, indicating that

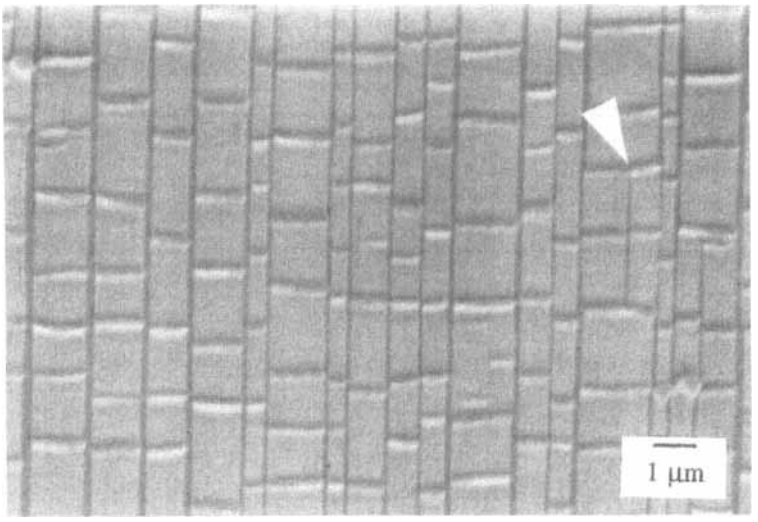

FIGURE 2 Fragmentation of the thick glass coating into parallel strips after application of a strain of 0.2. The arrow indicates an incomplete crack inside a strip.

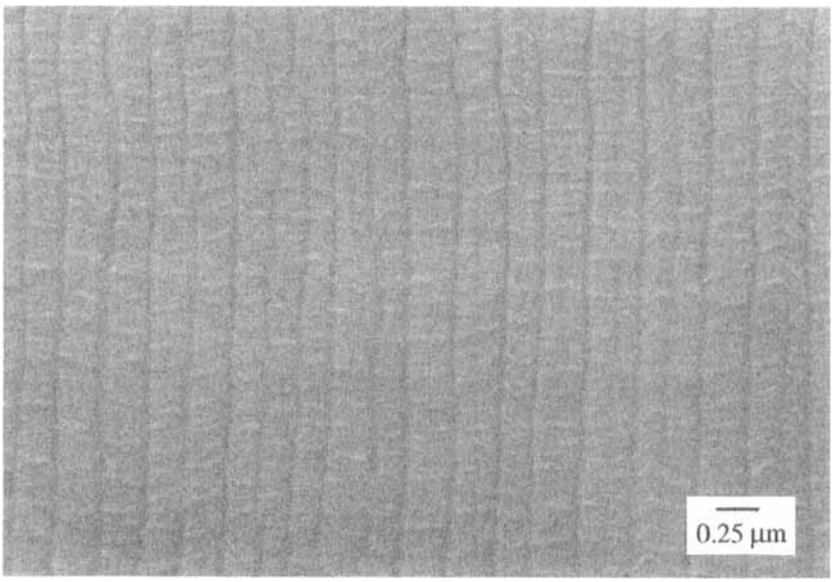

FIGURE 3 Fragmentation of the thin glass coating into parallel strips after application of a strain of 0.2. The tension direction is as shown on Figure 2.

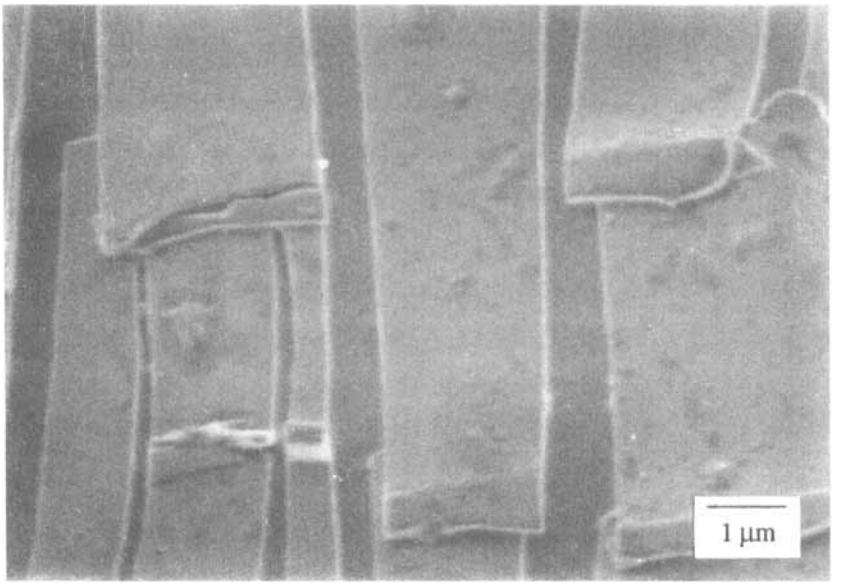

FIGURE 4 Overlapping glass fragments resulting from the compression of the coating strips during the straining of the film. The tension direction is as shown of Figure 2.

either the test was stopped before the completion of the fragmentation process, or some delamination of the strip edge occured, that stopped the fragmentation process.

Crack Spacing Distribution at Saturation

The spacing of the primary cracks after the crack density has reach its saturation value was measured from SEM images, chosen arbitrarily at several locations on the strained films. As mentioned previously, a few strips had not completed their fragmentation process. In order to correct for this effect in the calculation of the distribution, the incomplete fragmentations, as shown in Figure 2, were artificially completed by continuing the crack parallel to the strip direction. The distributions for the thick and thin sides are depicted in Figures 5 and 6, respectively. Statistical calculations for each distribution are reported in Table II. An interesting result is the ratio of the mean crack spacing, equal to 4.31. This value is within the experimental uncertainty of the ratio in thicknesses calculated previously.

DISCUSSION

The fragmentation pattern obtained after straining PET/glass coated specimens resembles that obtained in the classical single fiber fragmentation test.[23] In fiber reinforced composites, common stress transfer analyses relate the interfacial shear stress and the fiber strength to the critical fragmentation length, l_c and, therefore, the

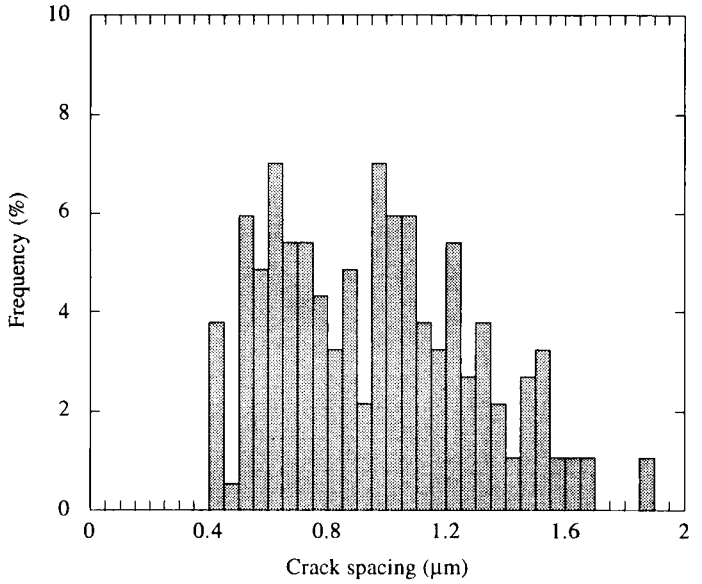

FIGURE 5 Crack spacing distribution at saturation after fragmentation of the thick glass coating.

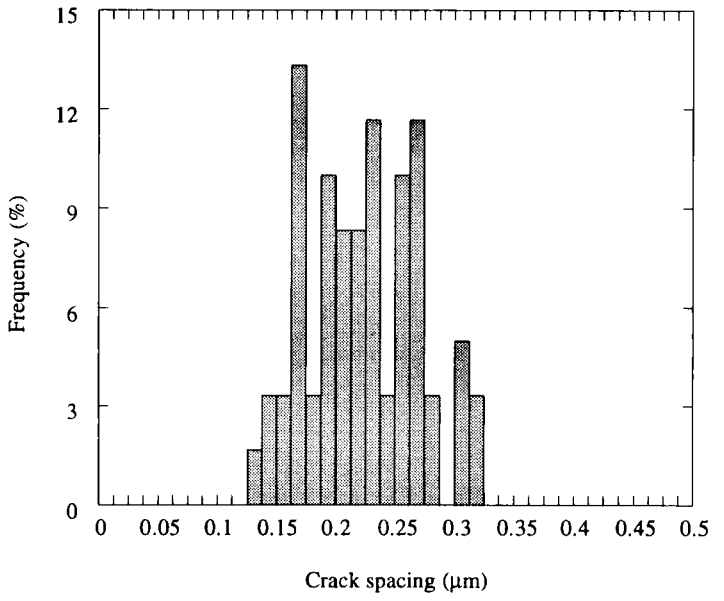

FIGURE 6 Crack spacing distribution at saturation after fragmentation of the thin glass coating.

TABLE II
Parameters of the crack spacing distribution at saturation

Glass coating side	Minimum (μm)	Maximum (μm)	Mean (μm)	Std. deviation (μm)
Thick (24 nm)	0.401	1.864	0.961	0.336
Thin (6 nm)	0.133	0.324	0.223	0.046

measurement of l_c leads to the determination of the interfacial shear strength,[24,25,28] providing that viscoelastic effects are small.[38] In the case of thin coatings on ductile substrates, successful modeling by Aveston and Kelly,[30] and Hu and Evans,[20] have also shown that the fragmentation process is governed by the stress transfer ability of the interface. A tensile load, applied to the specimen, is transferred from the substrate to the coating, and it provokes the progressive fragmentation of the coating until a critical crack density is reached. Furthermore, it has been shown recently that the reversible work of adhesion is directly proportional to the interfacial shear strength.[31-33] Following these approaches, a method has been derived to calculate the interfacial adhesion of the glass coating on the PET substrate.

Stress Transfer Analysis in the Polymer/Glass Bilayered Structure

The stress distribution at the interface and in the glass layer is calculated from the equilibrium of a small element of the glass layer subjected to a tension force parallel to the interface, as depicted in Figure 7. The equilibrium of an infinitesimal glass slice of thickness, h_g, length, dx, and width, L, requires:

$$Lh_g\sigma_g + Ldx\tau = Lh_g(\sigma_g + d\sigma_g) \tag{2}$$

where σ_g is the glass layer stress along the loading direction x, and τ is the interfacial shear stress. The equilibrium balance is rewritten as:

$$\frac{d\sigma_g}{dx} = \frac{\tau}{h_g}. \tag{3}$$

According to previous analysis [23,24] equation (3) was integrated with the following assumptions.

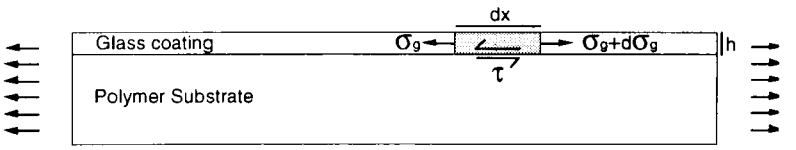

FIGURE 7 Equilibrium of an infinitesimal glass slice of length, dx, and thickness, h, along the loading direction.

i) The end effects on the glass layer are negligible. This is usually considered because of yielding of the substrate adjacent to the coating ends,[24,27] and also because the coating edge is not in contact with the polymer substrate.
ii) The PET matrix is perfectly plastic (*i.e.*, the interfacial shear strength is constant). This assumption relies on the mechanical data previously shown, as from the fact that the yield strain of PET (around 3%, Table I) is lower than the glass elongation at fracture.[37] Further work is being carried out to examine the fragmentation kinetics, with particular attention paid to the onset and saturation strain limits of the fragmentation process.
iii) The coating strength, σ_{max}, is independent of the fragment size.

The resulting coating stress evolution is linear with the coordinate x and a critical crack spacing l_c is defined as the minimum coating length in which the maximum allowable coating stress, σ_{max}, can be achieved:

$$l_c = 2h_g \frac{\sigma_{max}}{\tau} \tag{4}$$

This result is identical to the solution obtained by Hu and Evans[20] in their calculation of the crack energy release rate for very thin films. The theoretical crack spacing distribution has been modeled in numerous situations, as detailed in recent works examining the simple fiber fragmentation test.[39,40] We have followed a stochastic procedure,[41] and the resulting distributions are depicted on Figures 8 and 9, together with the experimental distributions, for the thick and thin coatings, respective-

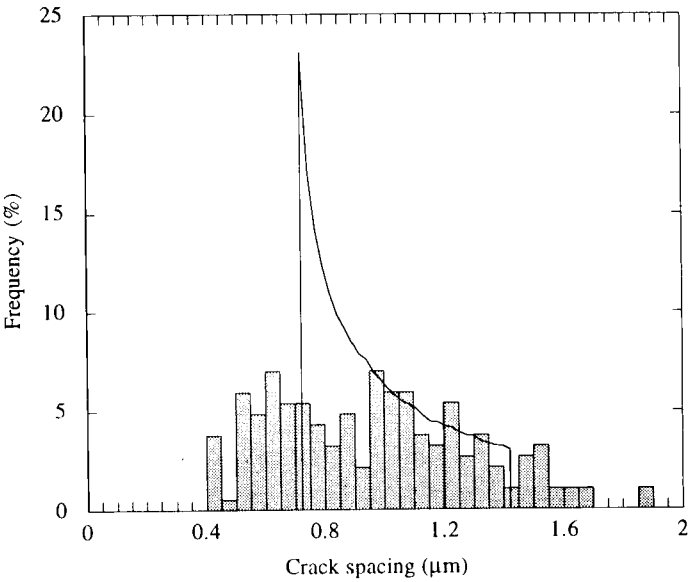

FIGURE 8 Theoretical crack spacing distribution at saturation assuming a trapezoidal stress profile in the coating, and a unique coating strength (line), compared with the experimental distribution, in the case of the thick coating.

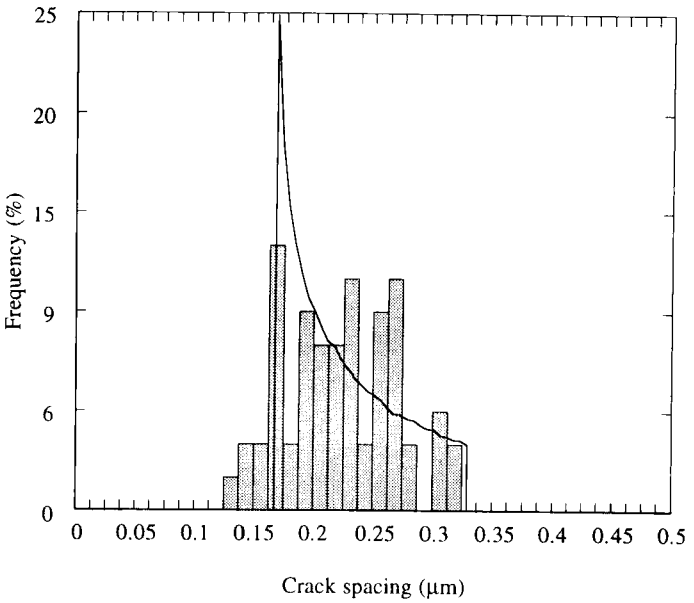

FIGURE 9 Theoretical crack spacing distribution at saturation assuming a trapezoidal stress profile in the coating, and a unique coating strength (line), compared with the experimental distribution, in the case of the thin coating.

ly. This model indicates that the crack spacings are distributed in the range between $l_c/2$ and l_c, and the exact calculation gives the mean crack spacing $\bar{l} = 1.337\, l_c/2$[42], that is closer to $l_c/2$ than to l_c, as reported in various works.[30,41] This result contradicts some authors assuming an even distribution of the fragment sizes between $l_c/2$ and l_c, yielding an average value $\bar{l} = 3/4\, l_c$.[26,27] Although the hypothesis of a unique coating strength may be crude, the theoretical distributions fit roughly the experimental distributions, and are far from being even in the range $l_c/2$ to l_c (Figs. 8 and 9). Moreover, even though the experimental distributions are slightly broader than from $l_c/2$ to l_c, the mean value 0.6685 l_c should be still valid, especially since high adhesion levels are achieved with CVD, therefore limiting the dispersion of the distribution.[41]

Furthermore, the theory predicts that the ratio of $\bar{l}$ between the thick and thin coatings should be equal to the ratio in thicknesses. This was found experimentally to be almost the case, the ratios differing by only 7%, which is within the experimental uncertainty of 14%. Consequently, no further refinement appears to be relevant to describe the coating strength (*e.g.*, Weibull distribution[43,44]).

Considering these results, an expression for the interfacial shear strength, τ, is derived from equation (4):

$$\tau = 1.337\, h_g \frac{\sigma_{max}}{\bar{l}} \tag{5}$$

Equation (5) shows that τ is proportional to $h_g/\bar{l}$. Consequently, considering the above remark, the calculated values reported in Table III are close to each other. This is

TABLE III
Interfacial shear strengths of CVD glass coatings on a PET substrate

Glass coating side	Thickness h (nm)	Strength, σ_{max} (MPa)	Mean spacing (μm)	Interfacial shear strength (MPa)
Thick	24	3000	0.961	100
Thin	6	3000	0.223	108

expected since both coatings were deposited during the same operation, and tested on the same film specimen. This result is clearly significant of the efficiency of the shear-lag analysis in the case of our material system.

Adhesive Pressure and Adhesion Energy

In a recent work, Schultz and Nardin[31] showed that a proportional relationship exists between the interfacial shear strength, τ, measured by the fragmentation test described in the preceding section, and the reversible work of adhesion, W, at the coating/substrate interface. Such a relationship assumes that only physical bonds are present at the interface, and that the coating does not modify the local properties of the polymer substrate. However, the authors consider the very probable existence of an interphase layer, the properties of which may differ significantly from those of the substrate.[32] Therefore one has:

$$\tau = kW \tag{6}$$

An interpretation of the analytical model of Cox[29] regarding the interfacial stress transfer led to an expression of the slope, k, based on the elastic properties of the components involved in the stress transfer. Equation (6) is rewritten as follows:

$$W = \delta^{-1}(E_g/E_p)^{1/2}\tau \tag{7}$$

where δ^{-1}, which is a constant independent of the system studied,[32,33] is a distance close to 0.5 nm, E_g and E_p are the elastic moduli of the glass coating and the polymer substrate, respectively, calculated in the preceding section. Although equation (7) was developed in the case of pure elastic stress transfer, we assume that it should hold even if the polymer substrate attains the plastic regime, for two main reasons. Firstly, the work of adhesion is related to a short interaction distance of 0.5 nm, typical of the interfacial bonds length. Since the SiO_2 coating may be considered as an elastic medium, the interfacial interactions will be locally subjected to an elastic field as the film is loaded. This assumption is valid until adhesive failure (*i.e.*, interfacial delamination) occurs which, in the present case, was observed beyond the saturation limit for the fragmentation (Fig. 4). Secondly, it is now well established that the fundamental mechanisms of plasticity in polymers are connected to the elastic properties, and involve localized mobility.[45,46] For instance, anelasticity results from stress activation of local defect areas, and plasticity results from the coalescence of these defect zones.[46] Interfacial bonding of the PET to the SiO_2 obviously prevents the activation and coalescence of

TABLE IV
Adhesion performance of glass CVD coatings on a PET substrate

Glass coating side	Coating thickness (nm)	Interfacial shear strength (MPa)	Adhesion pressure (MPa)	Adhesion energy (mJ/m^2)
Thick	24	100	442	221
Thin	6	108	477	238

the above mechanisms. Therefore, the elastic modulus of the polymer was found to be the relevant parameter in the calculation. A detailed analysis of the microscopic mechanisms related to the stress transfer would be needed to confirm the validity of the above treatment, which is open to discussion. The term $(E_g/E_p)^{1/2}\tau$ in equation (7) corresponds to a normalized interfacial strength considered as an interfacial pressure.[32,33] The adhesion pressures and adhesion energies for both the thick and the thin coatings are calculated using equation (7), and reported in Table IV. As previously pointed for the interfacial shear strength, the values of the adhesion energy are close to one another for both coatings. Interestingly, these values are in good agreement with the estimated work of adhesion at the SiO_2/PMMA interface, close to $225\,mJ/m^2$.[47] These high adhesion levels may be related to strong specific interactions, such as hydrogen bonds, established between silanol groups of silica and oxygen-containing carboxyl groups of the polymer. It has been shown that the acid-base interactions nearly double the work of adhesion of basic polymers to silica,[47] and it may be considered to a first approximation that PET presents a basic character similar to that of PMMA, although the aromatic rings of PET could play an important role in acid-base interactions. Further, this reflects the efficiency of the CVD process in yielding very high adhesion levels.

CONCLUSIONS

A simple and reliable adhesion test of thin, hard coatings on a polymer substrate was presented. In this technique, inspired by the mechanics of rupture of brittle films on elongated substrates, specimens are strained under uniaxial tension, leading to multiple fragmentations of the coating. A classical shear-lag analysis at the coating/substrate interface links the fragmentation pattern parameters to the interfacial shear strength and the reversible adhesion energy. Fragmentation tests carried out on a PET film coated on both sides by SiO_2 layers (24 nm on the thick side, and 6 nm on the thin side), led to the following conclusions:

1. Both the thick and thin coatings exhibit similar fragmentation patterns, upon straining up to 20%, with parallel cracks perpendicular to the loading direction. The tension exerted on the specimens provokes a compression of the parallel strips which break into rectangular fragments.
2. The difference between the ratio in mean crack spacing and the ratio in thickness for the thick and thin coatings is within the experimental uncertainty. This result

strongly suggests that the shear-lag analysis assuming a unique coating strength is relevant in the case of the present material system.

3. The interfacial shear strength is close to 100 MPa for both coatings. The adhesion energy of SiO_2 on PET is of the order of 230 mJ/m^2. Both values are slightly higher for the thin coating side.

Acknowledgements

The authors are indebted to the Council of the Swiss Federal Institute of Technology for supporting this work through the Materials Priority Program, and to Pharmacia Hospital Care for their support. They wish to thank Dr. J. T. Felts of Airco Coating Technology for supplying film samples and Dr. S. Toll of the Laboratoire de Technologie des Composites et Polymères of the Ecole Polytechnique Fédérale de Lausanne for the calculation of the theoretical crack spacing distributions.

References

1. J. T. Felts, *Proc. 3rd Int. Conf. Vac. Web Coatings*, Nov. 12–14, 1989, San Antonio, TX, USA.
2. J. T. Felts and A. D. Grubb, *J. Vac. Sci. Technol.* **A10**, 1675 (1992).
3. J. T. Felts, *Transparent barrier coating update: flexible substrates*, internal publication, Airco Coating Technology (1993).
4. D. S. Campbell, in *Handbook of thin film technology*, L. I. Maissel and R. Glang, Eds. (McGraw Hill, New York, 1970).
5. B. N. Chapman, *J. Vac. Sci. Technol.* **11**, 106 (1974).
6. K. L. Mittal, *Electrocomponent Sci. Technol.* **3**, 21 (1976).
7. J. Valli, *J. Vac. Sci. Technol.* **A4**, 3007 (1986).
8. K. L. Mittal, *J. Adhesion Sci. Technol.* **1**, 247 (1987).
9. P. A. Steinmann and H. E. Hintermann, *J. Vac. Sci. Technol.* **A7**, 2267 (1989).
10. P. R. Chalker, S. J. Bull and D. S. Rickerby, *Mat. Sci. Eng.* **A140**, 583 (1991).
11. S. Ramaligan, *Thin Sol. Films* **118**, 335 (1984).
12. G. M. Pharr and W. C. Oliver, *MRS Bulletin*, 28 (1992).
13. A. Kulik, J. -E. Bidaux, G. Gremaud and P. Bujard, in *Acoustic sensing and probing*, A. Alippi, Ed. (World Scientific, London, 1992), p. 419.
14. M. Urchulutegui, J. Piqueras and J. Lopis, *J. Appl. Phys.* **181**, 2677 (1989).
15. A. Brigg, *Acoustic microscopy* (Clarendon Press, Oxford, 1992), p. 224.
16. T. S. Chow, C. A. Liu and R. C. Penwell, *J. Polym. Sci., Polym. Phys. Ed.* **14**, 1305 (1976).
17. K. L. Mittal Ed., *Adhesion measurement of thin films, thick films, and bulk coatings* (ASTM, Philadelphia, 1978).
18. M. D. Thouless, *Thin Sol. Films* **181**, 397 (1989).
19. P. H. Wojciechowski and M. S. Mendolia, *J. Vac. Sci. Technol.* **A7**, 1282 (1989).
20. M. S. Hu and A. G. Evans, *Acta Metall.* **37**, 917 (1989).
21. D. C. Agrawal and R. Raj, *Acta Metall.* **37**, 1265 (1989).
22. P. H. Wojciechowski and M. S. Mendolia, in *Physics of thin films*, M. H. Francombe and J. L. Vossen, Eds. (Academic Press, New York, 1992), p. 271.
23. A. Kelly and W. R. Tyson, *J. Mech. Phys. Sol.* **13**, 329 (1965).
24. B. D. Agarwal and L. J. Broutman, *Analysis and performance of fiber composites* (John Wiley and Sons, New York, 1990), Chap. 4, p. 122.
25. M. Miwa, T. Oshawa, and K. Tahara, *J. Appl. Polym.* Sci. **25**, 795 (1980).
26. T. Oshawa, A. Nakayama, M. Miwa and A. Hasegawa, *J. Appl. Polym.* Sci. **22**, 3203 (1978).
27. L. Dilandro, A. T. Dibenedetto and J. Groeger, *Polym. Compos.* **9**, 209 (1988).
28. E. L. Asloun, M. Nardin and J. Schultz, *J. Mater. Sci.* **24**, 1835 (1989).
29. H. L. Cox, *Br. J. Appl. Phys.* **3**, 72 (1952).
30. J. Aveston and A. Kelly, *J. Mater. Sci.* **8**, 352 (1973).
31. J. Schultz and M. Nardin, in *Controlled interphases in composite materials*, H. Ishida, Ed. (Elsevier, New York, 1990), p. 561.
32. M. Nardin, E. M. Asloun and J. Schultz, *Polym. Adv. Technol.* **2**, 115 (1991).
33. M. Nardin and J. Schultz, *Compos. Interfaces* **1**, 177 (1993).

34. P. Bradley, *Caractérisation du revêtement et de l'interface d'un film SiO_x/PET de l'industrie de l'emballage*, to be published.
35. N. P. Bansal and R. H. Doremus, *Handbook of glass properties* (Academic Press, New York, 1986), p. 16.
36. J. A. Brydson, *Plastic materials* (Butterworths, London, 1989).
37. M. Grayson, *Encyclopedia of glass, ceramics, and cement* (John Wiley and Sons, New York, 1985), p. 492.
38. L. Monette, M. L. Anderson and G. S. Grest, *Polym. Compos.* **14**, 101 (1993).
39. T. Lacroix, B. Tilmans, R. Keunigs, M. Desaeger and I. Verpoest, *Compos. Sci. Technol.* **43**, 379 (1992).
40. P. Feillard, Ph. D. Thesis, INSA, France, (1993).
41. W. A. Fraser, F. H. Ancker, A. T. Dibenedetto and B. Elbirli, *Polym. Compos.* **4**, 238 (1983).
42. A. C. Kimber and J. G. Keer, *J. Mater. Sci. Letters* **1**, 353 (1982).
43. W. Weibull, *J. Appl. Mech.* **18**, 293 (1951).
44. E. L. Asloun, J. B. Donnet, G. Guilpain, M. Nardin and J. Schultz, *J. Mater. Sci.* **24**, 3504 (1989).
45. D. Hentschel, H. Sillescu and H. W. Spiess, *Polymer* **25**, 1078 (1984).
46. N. Ouali, M. B. M. Mangion and J. Perez, *Philos. Mag.* **67**, 827 (1993).
47. F. M. Fowkes, D. W. Dwight, D. A. Cole and T. C. Huang, *J. Non-Cryst. Sol.* **120**, 47 (1990).